Improvement of a Low Cost MEMS-based GPS/INS, Micro-GAIA

*Takeshi Fujiwara[1], Toshiaki Tsujii[1], Hiroshi Tomita[1], Masatoshi Harigae[1]

[1]Aviation Program Group, Japan Aerospace Exploration Agency
(E-mail: fujiwara.takeshi@jaxa.jp)

Abstract

Recently, inertial sensors like gyros and accelerometers have been quite miniaturized by Micro Electro-Mechanical Systems (MEMS) technology. JAXA is developing a MEMS-based GPS/INS hybrid navigation system named Micro-GAIA. The navigation performance of Micro-GAIA was evaluated through off-line analysis by using flight test data. The estimation errors of the roll, pitch, and azimuth were 0.03°, 0.05°, and 0.33° (1σ), respectively. The horizontal position errors after 60-second GPS outages were reduced to 25 m CEP. The attitude errors and position errors are nearly half of ones reported previously[2]. Furthermore, using the adaptive Kalman filters, the robustness against the uncertainty of the measurement noise was improved. Comparing the innovation-based and residual-based adaptive Kalman filters, it was confirmed that the latter is robuster than the former.

Keywords: GPS/INS, Hybrid Navigation, MEMS, Adaptive Kalman Filter, Flight Test

1. Introduction

JAXA developed a high-precision GPS/INS hybrid navigation system named GAIA, GPS Aided Inertial navigation Avionics[1]. Recently, inertial sensors such as gyros and accelerometers have been quite miniaturized by Micro Electro-Mechanical Systems (MEMS) technology. JAXA is now developing a MEMS-based GPS/INS hybrid navigation system, Micro-GAIA. Owing to its small size, light weight, and low cost realized by the MEMS technology, the utilization of high-precision navigation systems can be extended to small aircraft, e. g., general aviation and unmanned aerial vehicles.

Concerning a GPS/INS hybrid navigation system, when GPS aid is unavailable due to GPS signal blockages and others, the Inertial Measurement Unit (IMU) is used as a stand-alone navigation system. Although MEMS-based inertial sensors are quite low cost, their errors such as gyro drifts and accelerometer biases are much larger. Therefore, a MEMS-based IMU degrades its positioning accuracy rapidly during GPS outages. As for ground application, it was reported that introducing vehicle motion constraints improves navigation performance, especially stand-alone inertial navigation performance[3]. However, these constraints are not applicable to aviation application. As for the aviation application, GPS signal blockages may not occur frequently because there are not trees, tunnels, nor tall buildings in the sky. However, the attitude maneuver of the airplane can induce the interruption of receiving the GPS signal. Since the requirement of reliability is much higher for the aviation application, it is important to guarantee the positioning accuracy during GPS outages.

We reported prototype development and its flight evaluation results[2]. Afterwards, various error factors of a MEMS-based IMU had been investigated in detail. Then, modifications were applied to suppress the positioning errors during GPS outages. Furthermore, to improve robustness against the uncertainty of the measurement noise, two types of adaptive Kalman filters were applied; the innovation-based adaptive filter and residual-based one.

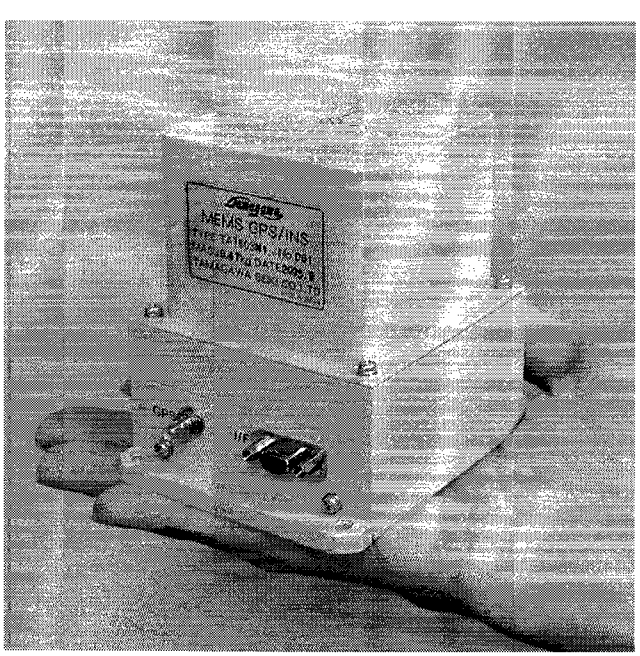

Figure 1. Micro-GAIA — MEMS-based GPS/INS

2. Micro-GAIA

Micro-GAIA is a MEMS-based GPS/INS hybrid navigation system as shown in figure 1, whose specifications are summarized in

Table 1. Specifications of Micro-GAIA

Model	TA7803N1
Accelerometer	
Range	±5 G
Scale Factor	±1 %
Bias Repeatability	±0.15 m/s^2
Gyro	
Range	±300°/s
Scale Factor	±0.5 %
Bias Repeatability	±0.2°/s
GPS	
Channel	12
Data Rate	1 Hz
Physical Characteristics	
Size	70 × 80 × 95 mm^3
Weight	470 g
Input Voltage	28 V

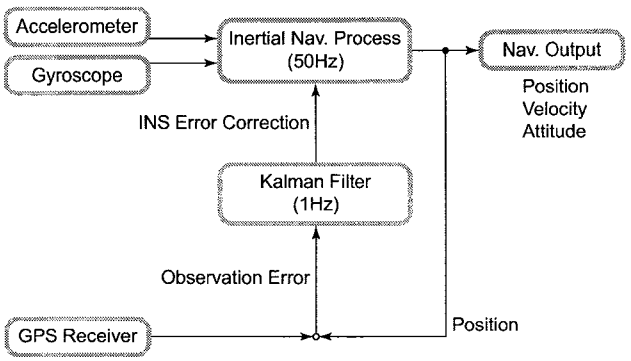

Figure 2. Navigation Algorithm

Table 2. State Variables in EKF

State	Number
Position Error	3
Velocity Error	3
Attitude Error	3
Accelerometer Bias	3
Gyro Bias	3
Total	15

table 1. It is being developed in JAXA for the aviation application, especially for small aircraft such as general aviation and unmanned aerial vehicles.

The navigation algorithm installed in Micro-GAIA can estimate 15 state variables listed in table 2 by using the Extended Kalman Filter (EKF) as shown in figure 2. Because the internal miniature GPS receiver in Micro-GAIA can output only positioning data, a loose-coupled filter is implemented, which compensates the INS errors by using GPS positioning data.

3. Problem Formulation

In this section, two types of adaptive measurement noise matrix estimation methods are derived from the measurement update equations of the conventional Kalman filter.

3.1 Measurement Update in the Kalman Filter

Only the measurement update in the Kalman filter is discussed in this section. Assuming all variables come from the same time-step, subscripts denoting time-step like k of $\boldsymbol{x}_k$ are omitted.

The estimated state vector $\widehat{\boldsymbol{x}}^-$ has the state estimation error vector $\delta\widehat{\boldsymbol{x}}^-$ relative to the true state vector $\boldsymbol{x}$, as

$$\delta\widehat{\boldsymbol{x}}^- = \widehat{\boldsymbol{x}}^- - \boldsymbol{x} \tag{1}$$

where a hat (circumflex) over a variable denotes an estimate of the variable. Additionally, superscript "$-$" denotes the estimate before the measurement update. The covariance matrix of $\delta\widehat{\boldsymbol{x}}^-$ is

$$\widehat{\boldsymbol{P}}^- = E\left[\delta\widehat{\boldsymbol{x}}^-(\delta\widehat{\boldsymbol{x}}^-)^T\right] \tag{2}$$

The measurement equation is defined as

$$\boldsymbol{y} = \boldsymbol{h}(\boldsymbol{x}) + \boldsymbol{v} \tag{3}$$

where $\boldsymbol{y}$ is the measurement vector, $\boldsymbol{v}$ is the zero-mean measurement noise vector, and $\boldsymbol{h}(\cdot)$ is the observation function relating the state to the measurement. The covariance matrix of $\boldsymbol{v}$ is

$$\boldsymbol{R} = E\left[\boldsymbol{v}\boldsymbol{v}^T\right] \tag{4}$$

and $\boldsymbol{v}$ does not have correlation with $\delta\widehat{\boldsymbol{x}}^-$,

$$E\left[\delta\widehat{\boldsymbol{x}}^-\boldsymbol{v}^T\right] = \boldsymbol{O} \tag{5}$$

The measurement update equations in the Kalman filter are described as follow:

$$\widehat{\boldsymbol{x}}^+ = \widehat{\boldsymbol{x}}^- + \boldsymbol{K}\left\{\boldsymbol{y} - \boldsymbol{h}(\widehat{\boldsymbol{x}}^-)\right\} \tag{6}$$

$$\widehat{\boldsymbol{P}}^+ = (\boldsymbol{I} - \boldsymbol{K}\boldsymbol{H})\widehat{\boldsymbol{P}}^- \tag{7}$$

where superscript "+" denotes the estimate after the measurement update. The observation matrix $\boldsymbol{H}$ is the Jacobian of the observation function $\boldsymbol{h}(\cdot)$,

$$\boldsymbol{H} = \left.\frac{\partial \boldsymbol{h}}{\partial \boldsymbol{x}}\right|_{\boldsymbol{x}=\widehat{\boldsymbol{x}}^-} \tag{8}$$

The Kalman gain matrix $\boldsymbol{K}$ is determined from

$$\boldsymbol{K} = \widehat{\boldsymbol{P}}^-\boldsymbol{H}^T(\boldsymbol{H}\widehat{\boldsymbol{P}}^-\boldsymbol{H}^T + \boldsymbol{R})^{-1} \tag{9}$$

3.2 Innovation-based Adaptive Estimation of $\boldsymbol{R}$

If the information of the measurement noise matrix $\boldsymbol{R}$ is incomplete, $\boldsymbol{R}$ can be estimated adaptively by using the innovation sequence or the residual sequence[4]. The innovation sequence is the sequence of the innovation vector defined as

$$\Delta\boldsymbol{y}^- = \boldsymbol{y} - \boldsymbol{h}(\widehat{\boldsymbol{x}}^-) \tag{10}$$

and the residual sequence is the sequence of the residual vector defined as

$$\Delta\boldsymbol{y}^+ = \boldsymbol{y} - \boldsymbol{h}(\widehat{\boldsymbol{x}}^+) \tag{11}$$

Substituting equations (1) and (3) into equation (10), linearized with equation (8), and ignoring the higher order terms, the innovation vector is related to the state estimation error before the measurement update,

$$\Delta\boldsymbol{y}^- = -\boldsymbol{H}\delta\widehat{\boldsymbol{x}}^- + \boldsymbol{v} \tag{12}$$

The covariance matrix of $\Delta\boldsymbol{y}^-$ is obtained from equations (2), (4), and (5) as follows:

$$\begin{aligned}\boldsymbol{C}^- &= E\left[\Delta\boldsymbol{y}^-(\Delta\boldsymbol{y}^-)^T\right] \\ &= E\left[\boldsymbol{H}\delta\widehat{\boldsymbol{x}}^-(\delta\widehat{\boldsymbol{x}}^-)^T\boldsymbol{H}^T\right] + E\left[\boldsymbol{v}\boldsymbol{v}^T\right] \\ &= \boldsymbol{H}\widehat{\boldsymbol{P}}^-\boldsymbol{H}^T + \boldsymbol{R} \\ &= \widehat{\boldsymbol{D}}^- + \boldsymbol{R}\end{aligned} \tag{13}$$

where $\widehat{\boldsymbol{D}}^- = \boldsymbol{H}\widehat{\boldsymbol{P}}^-\boldsymbol{H}^T$ is the covariance of the expected measurement error due to the state uncertainty before the measurement update.

If the estimate of $\boldsymbol{C}^-$ is obtained, the measurement noise matrix $\boldsymbol{R}$ can be estimated as follows:

$$\widehat{\boldsymbol{R}} = \widehat{\boldsymbol{C}}^- - \widehat{\boldsymbol{D}}^- \tag{14}$$

The estimated innovation matrix $\widehat{\boldsymbol{C}}^-$ is obtained by averaging the previous innovation sequence over a window size N,

$$\widehat{\boldsymbol{C}}_k^- = \frac{1}{N}\sum_{i=k-N+1}^{k}\Delta\boldsymbol{y}_i^-(\Delta\boldsymbol{y}_i^-)^T \tag{15}$$

or recursively,

$$\widehat{\boldsymbol{C}}_k^- = \widehat{\boldsymbol{C}}_{k-1}^- + \frac{1}{N}\left\{\Delta\boldsymbol{y}_k^-(\Delta\boldsymbol{y}_k^-)^T - \widehat{\boldsymbol{C}}_{k-1}^-\right\} \tag{16}$$

The window size N is very application specific.

3.3 Residual-based Adaptive Estimation of R

A similar expression using the residual sequence instead of the innovation sequence can also be derived. The state estimation error vector and its covariance after the measurement update are

$$\delta\hat{\boldsymbol{x}}^+ = \hat{\boldsymbol{x}}^+ - \boldsymbol{x} \tag{17}$$

$$\hat{\boldsymbol{P}}^+ = E\left[\delta\hat{\boldsymbol{x}}^+(\delta\hat{\boldsymbol{x}}^+)^T\right] \tag{18}$$

where superscript $+$ denotes the estimate after the measurement update.

In the same way as the innovation vector, the residual vector is related to the state estimation error after the measurement update,

$$\Delta\boldsymbol{y}^+ = -\boldsymbol{H}\delta\hat{\boldsymbol{x}}^+ + \boldsymbol{v} \tag{19}$$

However, different from the innovation-based expression, $\delta\hat{\boldsymbol{x}}^+$ has correlation with $\boldsymbol{v}$,

$$E\left[\delta\hat{\boldsymbol{x}}^+\boldsymbol{v}^T\right] \neq \boldsymbol{O} \tag{20}$$

The reason is because the state vector is updated by using the measurement vector including the measurement noise $\boldsymbol{v}$.

Substituting equations (1), (10), and (17) into equation (6), $\delta\hat{\boldsymbol{x}}^+$ is related to the innovation vector as follows:

$$\delta\hat{\boldsymbol{x}}^+ = \delta\hat{\boldsymbol{x}}^- + \boldsymbol{K}\Delta\boldsymbol{y}^- \tag{21}$$

Substituting equations (12) and (21) into equation (19), the residual vector is related to the innovation vector as follows:

$$\begin{aligned}\Delta\boldsymbol{y}^+ &= -\boldsymbol{H}\delta\hat{\boldsymbol{x}}^- + \boldsymbol{v} - \boldsymbol{H}\boldsymbol{K}\Delta\boldsymbol{y}^- \\ &= (\boldsymbol{I} - \boldsymbol{H}\boldsymbol{K})\Delta\boldsymbol{y}^-\end{aligned} \tag{22}$$

The covariance matrix of $\Delta\boldsymbol{y}^+$ is obtained by using equation (13) as follows:

$$\begin{aligned}\boldsymbol{C}^+ &= E\left[\Delta\boldsymbol{y}^+(\Delta\boldsymbol{y}^+)^T\right] \\ &= (\boldsymbol{I} - \boldsymbol{H}\boldsymbol{K})E\left[\Delta\boldsymbol{y}^-(\Delta\boldsymbol{y}^-)^T\right](\boldsymbol{I} - \boldsymbol{H}\boldsymbol{K})^T \\ &= (\boldsymbol{I} - \boldsymbol{H}\boldsymbol{K})(\boldsymbol{H}\hat{\boldsymbol{P}}^-\boldsymbol{H}^T + \boldsymbol{R})(\boldsymbol{I} - \boldsymbol{H}\boldsymbol{K})^T \\ &= -\boldsymbol{H}\hat{\boldsymbol{P}}^+\boldsymbol{H}^T + \boldsymbol{R} \\ &= -\boldsymbol{D}^+ + \boldsymbol{R}\end{aligned} \tag{23}$$

where $\widehat{\boldsymbol{D}}^+ = \boldsymbol{H}\hat{\boldsymbol{P}}^+\boldsymbol{H}^T$ is the covariance of the expected measurement error due to the state uncertainty after the measurement update.

In a similar way to the innovation-based estimation, $\boldsymbol{R}$ can be estimated from the estimate of $\boldsymbol{C}^+$ as follows:

$$\hat{\boldsymbol{R}} = \widehat{\boldsymbol{C}}^+ + \widehat{\boldsymbol{D}}^+ \tag{24}$$

The estimated residual matrix $\widehat{\boldsymbol{C}}^+$ is obtained from the residual sequence by either of two equations below:

$$\widehat{\boldsymbol{C}}_k^+ = \frac{1}{N}\sum_{i=k-N+1}^{k}\Delta\boldsymbol{y}_i^+(\Delta\boldsymbol{y}_i^+)^T \tag{25}$$

$$\widehat{\boldsymbol{C}}_k^+ = \widehat{\boldsymbol{C}}_{k-1}^+ + \frac{1}{N}\left\{\Delta\boldsymbol{y}_k^+(\Delta\boldsymbol{y}_k^+)^T - \widehat{\boldsymbol{C}}_{k-1}^+\right\} \tag{26}$$

Comparing equations (14) and (24), both are very similar but not same. All covariance matrices in equations (14) and (24) must be positive definite. While the sum of two positive definite matrices is also positive definite, the remainder of them is not guaranteed to be positive definite due to estimation error. Therefore, it is expected that the residual-based adaptive estimation is more stable than the innovation-based one.

4. Tests and Results

4.1 Flight Tests

We had performed several flight tests last year by using JAXA's experimental airplane named MuPAL-α, Multi-Purpose Aviation Laboratory – Airplane, as shown in figure 3. Through these flight tests, the navigation performances of Micro-GAIA were evaluated under the actual flight conditions such as takeoff, landing, and turns. Micro-GAIA was loaded on MuPAL-α and its data was collected during the flight tests.

To compare with the performance reported previously[2], we selected the same flight data for the performance evaluation. The outlines of the flight tests are summarized as follow:

- Period: Sep. 26 to Oct. 6, 2005
- Locale: Hokkaido (42.5°N, 143.4°E), JAPAN
- Flight Time: 2 hours × 8 flights
- Situation: takeoff, cruise, turn, approach, and landing

As an example, the flight trajectory of the case F02 is shown in figure 4.

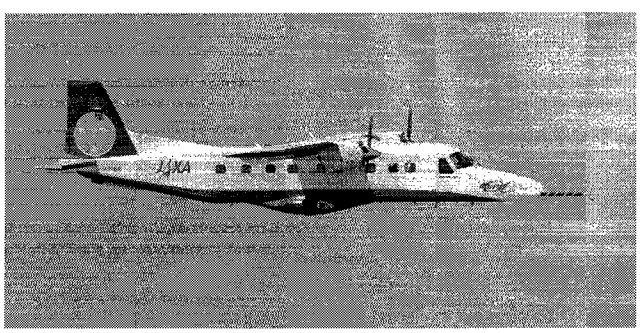

Figure 3. MuPAL-α, Experimental Airplane belonging to JAXA

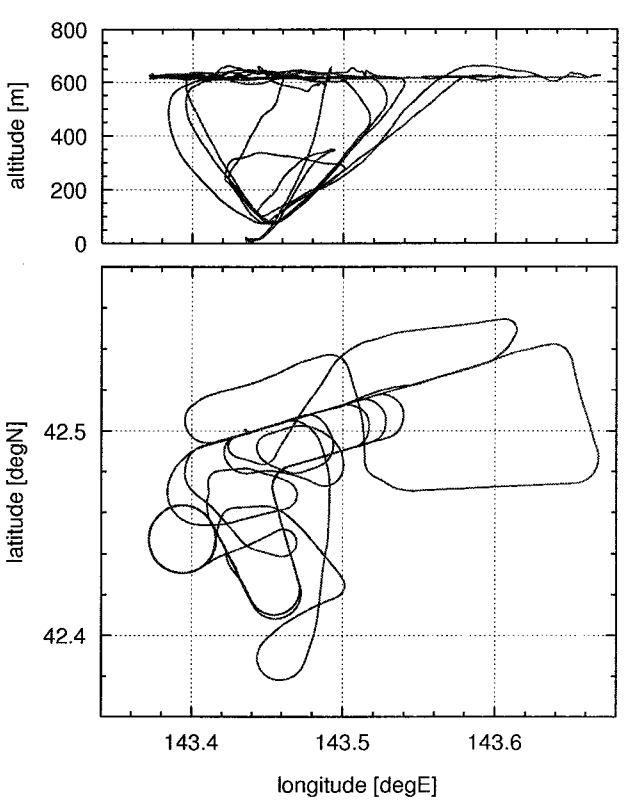

Figure 4. Flight Trajectory, Case F02, Sep. 28, 2005

Table 3. Parameters in Navigation Algorithm

Parameter	1σ
Observation Error	
Horizontal Position	0.02 m
Vertical Position	0.10 m
Initial Estimation Error	
Position	1.0 m
Velocity	1.0 m/s
Attitude	6.0 °
Acc. Bias	0.1 m/s^2
Gyro Bias	0.1 °/s
Acc. Error Parameters	
Noise (Random Walk)	1.0 m/s/$\sqrt{\text{h}}$
Bias Instability (1hr)	0.001 m/s^2
Scale Factor	1.0 %
Gyro Error Parameters	
Noise (Random Walk)	0.3 °/$\sqrt{\text{h}}$
Bias Instability (1hr)	0.02 °/s
Scale Factor	1.0 %

4.2 Navigation Performance

The navigation performance of Micro-GAIA under the flight condition was evaluated through the off-line analysis after the flight tests. Micro-GAIA data collected during the flight tests were processed with the parameters listed in table 3. While GPS data was available, the positioning accuracy of GPS/INS hybrid navigation depends on that of GPS. Therefore, the navigation performance was evaluated by investigating the attitude estimation accuracy. The attitude errors of Micro-GAIA compared to the reference attitude measured by a navigation grade GPS/INS are shown in figure 5 with blue lines while the uncertainty equivalent to 1σ is indicated by red lines. The estimation errors of the roll, pitch, and azimuth were 0.03°, 0.05°, and 0.33° (1σ), respectively.

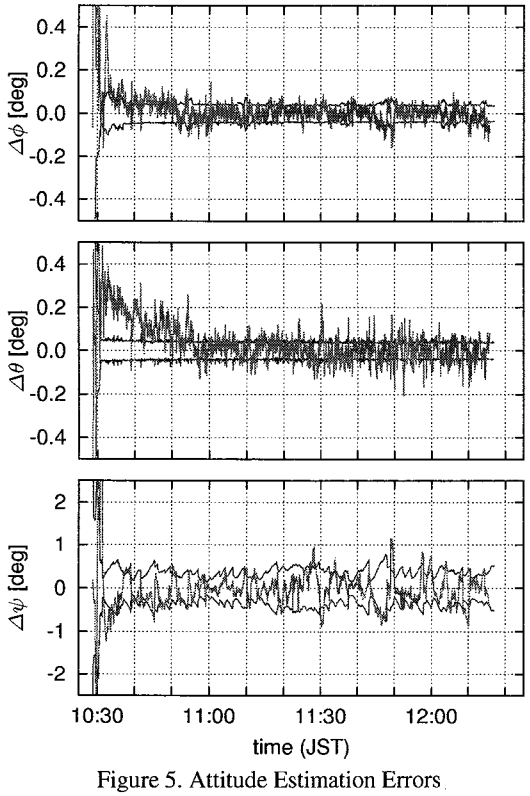

Figure 5. Attitude Estimation Errors

4.3 Coasting Performance

The navigation performance without GPS aid was evaluated by using the data including simulated GPS outages. The GPS outages were simulated by removing GPS data artificially from the actual flight data for a certain period. The duration of each GPS outage was fixed at 60 seconds.

The position errors of Micro-GAIA during GPS outages are indicated in figure 6. The time of the beginning of each GPS outage is arranged to $t = 0$. In the almost all cases, the position errors were less than 60 m.

The cumulative frequency of the horizontal position errors after 60-second GPS outages is shown in figure 7. It indicates that the circular error probability (CEP) was 25 m. These results were caused by several small improvements of the navigation algorithm and careful tuning of the navigation parameters.

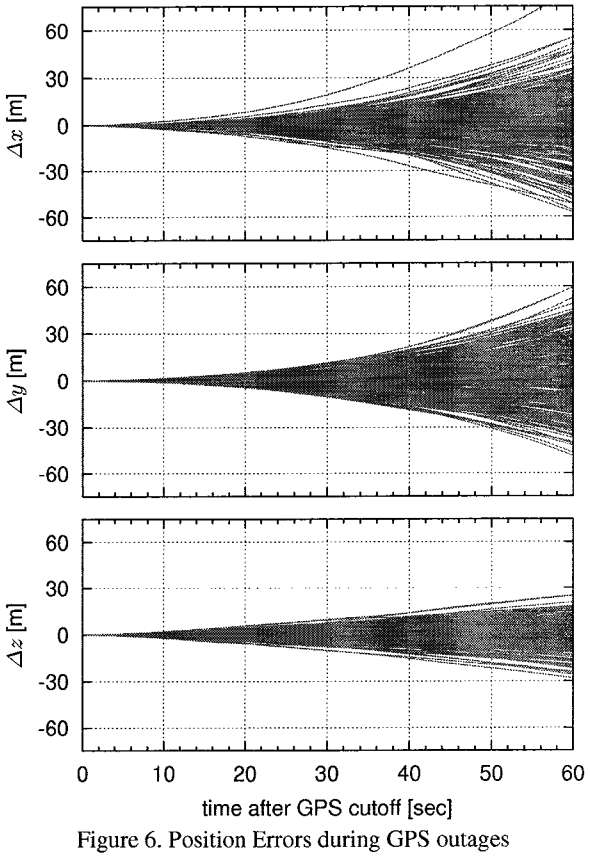

Figure 6. Position Errors during GPS outages

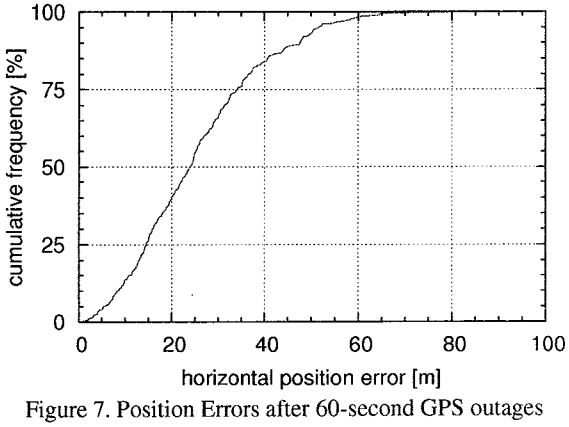

Figure 7. Position Errors after 60-second GPS outages

4.4 Adaptive Estimation of Measurement Noise

To improve robustness against the uncertainty of the measurement noise, two types of adaptive Kalman filters, the innovation-based adaptive filter and residual-based one, were applied. They were compared with the conventional Kalman filter, in which the measurement noise matrix $\boldsymbol{R}$ is constant.

The square roots of the diagonal components of the matrices in equation (14) or equation (24) are indicated in figures 8–10. $\boldsymbol{r}$ consists of the square roots of the diagonal components of $\boldsymbol{R}$, the given or estimated measurement error matrix. $\boldsymbol{d}$ consists of those of $\boldsymbol{D}$, the expected measurement error due to the state uncertainty.

Initially, both adaptive filters were given larger measurement noise matrices than that of the conventional filter. The estimates of the measurement noise matrices converged on reasonable values as mentioned later. As expected through the theoretical consideration, the convergence of the residual-based filter was more stable than that of the innovation-based one.

The navigation performances against the measurement noise matrix given to the filters at the beginning were investigated and shown in figure 11. From the results of the conventional filter, the actual measurement noise seemed to be a few centimeters. Because kinematic GPS positioning data were used as the measurement data in these Kalman filters, it can be said that the magnitude of the estimated measurement noise was reasonable.

In the case of the conventional filter, large measurement noise matrix caused large position errors. As for the innovation-based filter, small initial measurement noise matrix brought a divergence of the navigation process. Only the residual-based filter could keep the navigation performance through the wide range of the initial measurement noise matrices. It means that the residual-based filter has larger robustness against the uncertainty of the measurement noise than the others.

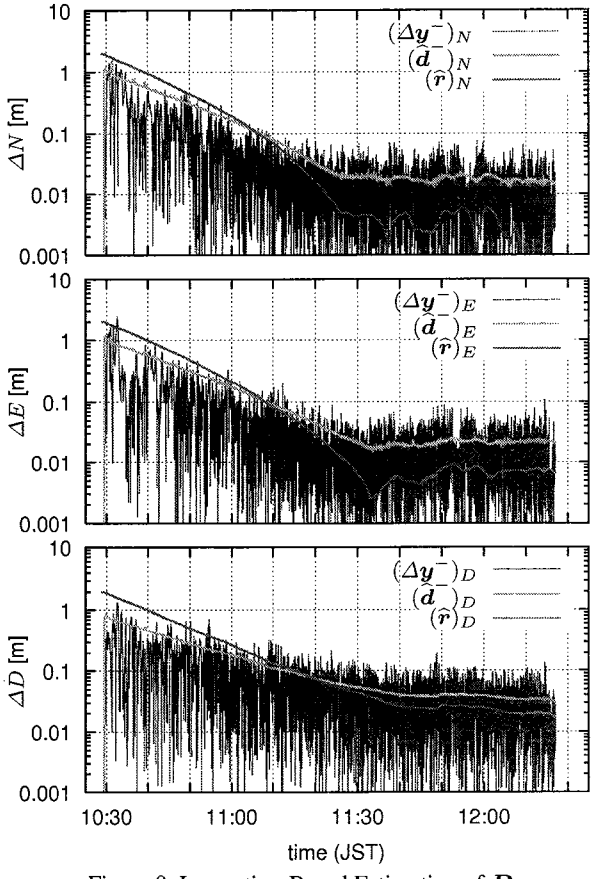

Figure 9. Innovation-Based Estimation of $\boldsymbol{R}$

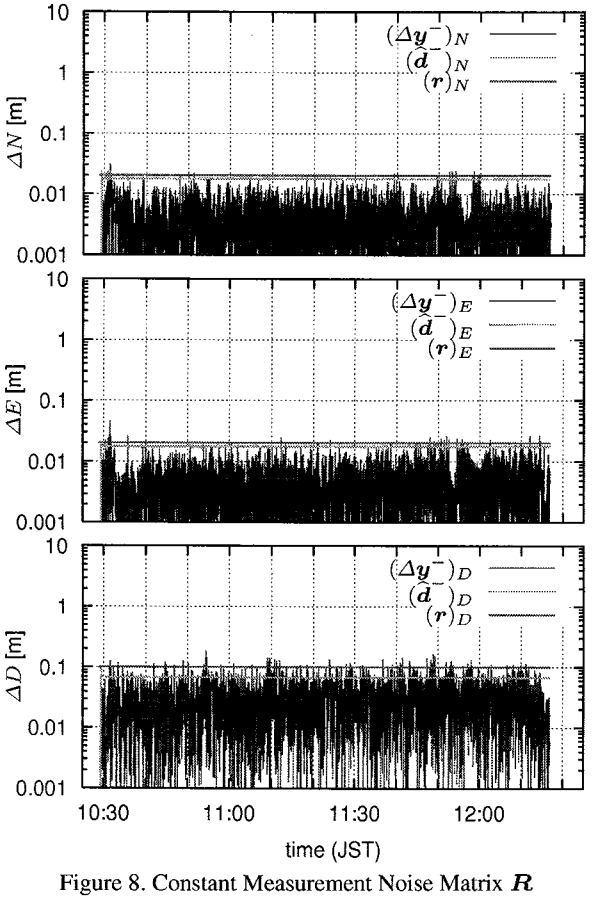

Figure 8. Constant Measurement Noise Matrix $\boldsymbol{R}$

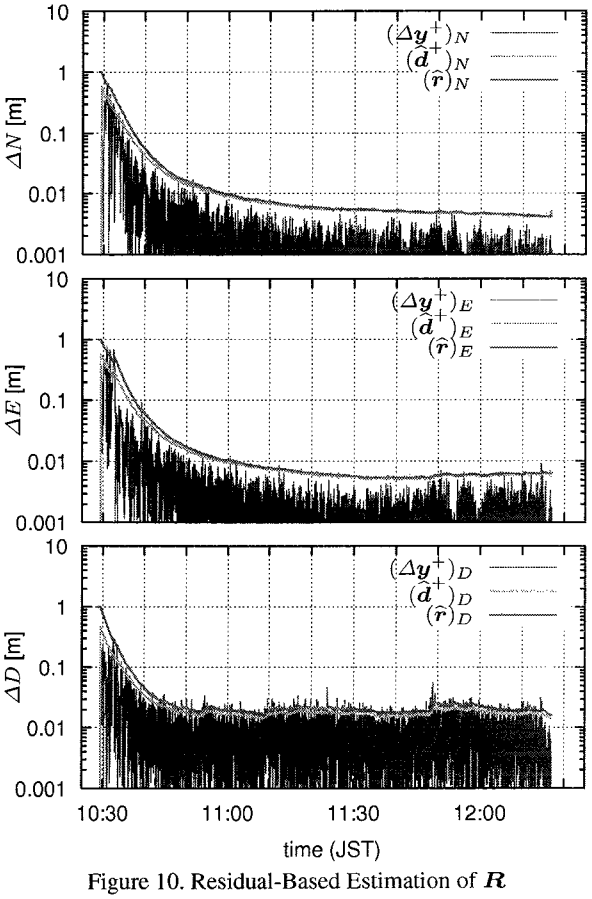

Figure 10. Residual-Based Estimation of $\boldsymbol{R}$

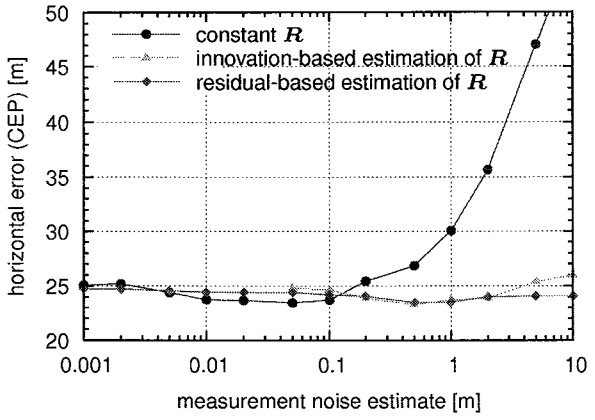

Figure 11. Sensitivity to Initial Estimate of $\boldsymbol{R}$

5. Conclusions

JAXA is developing Micro-GAIA, a MEMS-based GPS/INS hybrid navigation system. The navigation performance of Micro-GAIA was evaluated through the off-line analysis by using the flight test data. Because of several improvements of the navigation algorithm and careful tuning of the navigation parameters, the navigation accuracy was improved. The estimation errors of the roll, pitch, and azimuth were $0.03°$, $0.05°$, and $0.33°$ (1σ), respectively. The horizontal position errors after 60-second GPS outages were reduced from 40 m to 25 m CEP. The attitude errors and position errors are nearly half of ones reported previously[2].

Using the adaptive Kalman filters, robustness against the uncertainty of the measurement noise was improved. Comparing the innovation-based and residual-based adaptive Kalman filters, it was confirmed that the latter is robuster than the former. To raise the robustness higher, the adaptive estimation of the process noise matrix as well as the measurement noise matrix should be installed in future work.

Currently, a real-time onboard navigation software is just being developed. Some results of its onboard evaluation tests will be reported next time.

References

1. M. Harigae, H. Tomita, and T. Nishizawa, "Development of GPS Aided Inertial Navigation System for High Speed Flight Demonstrator," *Proceedings of ION GPS 2001*, Sep. 2001
2. T. Fujiwara, H. Tomita, T. Tsujii, and M. Harigae, "Development and Flight Evaluation of Micro-GAIA, MEMS GPS/INS Navigation System," *Proceedings of International Symposium on GPS/GNSS 2005*, Dec. 2005
3. S. Godha and M. E. Cannon, "Integration of DGPS with a Low Cost MEMS-Based Inertial Measurement Unit (IMU) for Land Vehicle Navigation Application," *Proceedings of ION GPS 2005*, Sep. 2005
4. A. H. Mohamed and K. P. Schwarz, "Adaptive Kalman Filtering for INS/GPS," *Journal of Geodesy*, 73:193–203, 1999